Estimations of Spatial Variability of Cone Resistance Using Geostatistical Method

지구통계학적 기법을 이용한 콘저항치의 공간적 변화의 평가

Yoon, Gil-Lim*[1]
윤 길 림
Michael, W. O'Neill*[2]

요 지

과압밀된 점토현장에서 수행한 콘관입시험 자료를 지구통계학 방법으로 분석하였다. 임의로 위치한 28개의 콘 사운딩 자료(A현장)와 일관되게 위치한 38개의 콘 사운딩 자료(B현장)분석에 이용되었다. 크리깅기법을 이용하여 두 현장의 콘 저항에 대한 베리어그램을 개발했다. 개발된 베리오그램은 현장에서의 수직적 상관거리 및 수평적 상관거리를 규명하는데 이용되었으며 이의 결과는 두 시험결과를 상호비교하려면 샘플링이 수평상관거리 이내에서 수행되어야하는 최적샘플링설계로 이용된다. 베리오그램의 분석결과는 두 현장의 지질학적 형성이 수직적 및 수평적으로 큰 차이가 없음을 확인할 수 있었다.

A현장에서의 크리깅한 콘 저항치를 3차원적으로 나타낸 표면은 콘 저항치의 공간적 변동을 이해하는데 도움을 주며 또한 지구통계학적으로 분석된 3차원적 표면은 분석된 현장의 어느 위치에서나 최적의 콘 저항치를 나타낼 수 있다는 것을 의미한다.

Abstract

Applications of geostatistical method to cone penetrometer data have been performed at the overconsolidated clay site. Randomly-located 28 electronic CPT soundings(Location A) and consistently-located 38 CPT soundings(Location B) are investigated geostatistically. Variograms for Locations A and B have been developed for q_c from the CPT data by using "kriging" principles, which establish the horizontal and vertical correlation distances at this site. These vertical and horizontal correlation distances can be used to optimal sampling design, where, if one needs to compare two test results, sampling must be made within these vertical and horizontal correlation distances. Analysis of the variograms indicated that the geological formation between two locations are not very different in both vertical direction and horizontal direction.

*[1] 정회원, 현대건설(주) 기술연구소

*[2] Professor, Department of Civil and Environmental Engineering, University of Houston, Houston, TX 77204-4791.

Kriged three-dimensional surfaces for Location A give a clear understanding of spatial variability of q_c, which suggests that geostatistical theory can be used to provide the most probable values of q_c in three dimension at any point on the site.

Keywords : Geostatistics, Kriging, CPT, In-situ test, Variogram, Spatial variability, Soil properties.

1. Introduction

In situ measurements of vertical and horizontal variations in soil properties using the cone penetration test(CPT) can provide useful information for stratigraphic interpretation on a site. In the analysis of CPT data, classical statistical methods such as regression or correlation analysis are occasionally used. However, these methods do not consider soil properties spatially, which may exhibit considerable variation naturally from one location to another(Lumb, 1966). Proper accounting for spatial variability when predicting geotechnical performance may reduce significantly the uncertainties associated in a particular design if variability characteristics of local soil conditions can be understood.

With the advent and wide application of geostatistics in the fields of geology, mining, and hydrogeology, geotechnical engineers have begun in recent years to appreciate its practical advantages(Soulie, 1983; Baecher, 1983; Christakos, 1985). However, not much work has been reported in the literature concerning application of geostatistics to site characterization of the spatial distribution of CPT data. Most geostatistical development so far has come from mining applications in which lack of sufficient three-dimensional data is rarely a problem.

In a recent study, Jaksa et al.(1993) modeled CPT data by geostatistics theory in order to estimate spatial correlation in the vertical direction and horizontal direction in a stiff, overconsolidated clay, similar to the Beaumont formation considered here. Tang(1979) evaluated horizontal correlation distance of CPT data using the autocorrelation function and Campanella and Wickremesinghe(1989) described the application of CPT data to site characterization using Vanmarke's variance function. These theories give an indication of the degree of variability of a profile and indicate the distance of perfect correlation from point to point(Vanmarke, 1977). Variance functions are related to variograms, which describe spatial autocorrelation between measurements at given locations(Ledvina, 1991).

This paper describes briefly techniques of geostatistics that have been used to analyze a large set of CPT data for estimating spatial variability of cone resistance(q_c) at the overconsolidated site.

2. Description of Test Site

The study site shown in Fig. 1 is the national geotechnical experimentation site located

on the University of Houston central campus in Houston, Texas(NGES-UH). It is situated on a series of unconformable Pleistocene-aged transported terrace deposits. Details of geological and engineering site descriptions are given by Mahar and O'Neill(1983) and O'Neill and Yoon(1996). The test site is essentially flat except for minor vertical relief on the extreme north end. The locations of the CPT soundings in Locations A and B are shown in Fig. 1.

Figure 2 shows the general stratigraphy of the upper two deposits investigated by an *in situ* and laboratory test program. The layers of interest here, marked 1, 2, and 3, are in the Beaumont formation, while those marked 4-8 are in the Montgomery formation. The Beaumont formation, extending from the surface to a depth of approximately 8m, was deposited in a deltaic environment during the Peorian Interglacial stage and preconsolidated by desiccation as the nearby sea withdrew during the late Wisconsin Ice Age. The formation has not been affected by any significant tectonic activity since deposition. The Beaumont formation is economically important because it is the primary foundation material for structures near the Gulf Coast from south-central Louisiana to south Texas.

The Beaumont soils are clays of high plasticity(CH) with a network of variable, closely spaced, discontinuous fissures and slickensides, which are inherent planes of weakness. Mahar and O'Neill(1983) hypothesized that there exists pointwise variability in preconsolidation pressure and shear strength in the soil due to cracks during desiccation.

In this paper only the Beaumont formation has been considered because much more extensive CPT data are available.

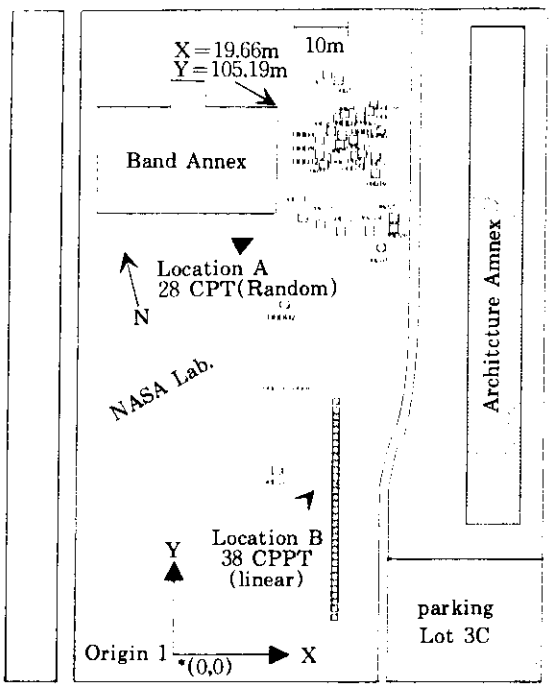

Fig.1 National geotechnical experimentation site at the University of Houston

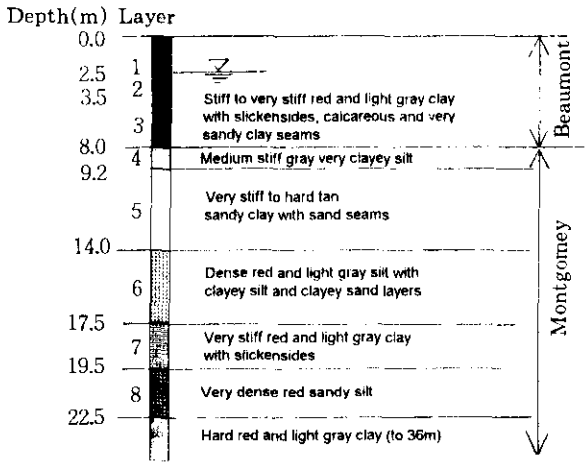

Fig.2 General stratigraphy of the NGES-UH site

3. CPT Data Set

There are two locations shown in Fig.1: Locations A and B. Location A is the site of numerous small foundation tests in the 1970s and 1980s. Fugro-type cone penetrometer soundings were made near each tested foundation, prior to construction, which resulted in a variation in location that will be considered here to be random. A total of 28 CPTs are available in that area. At Location B 38 additional soundings were made in a regular linear pattern(0.9 m horizontal distance) for the purpose of investigating horizontal correlation. All CPTs were made by using truck or drill rig reactions at penetration rates of 0.01-0.02 m/sec.

For each of the cone soundings, a continuous recording of the cone tip resistance(q_c) was taken. The q_c values to be used as estimates of the mean and coefficient of variation(COV) for each layer should be representative of the soil type through the entire layer of interest. Portions of the digitized records of q_c need to be pooled or averaged vertically, to compute mean and COV(Anderson et al., 1984). Pooling has been performed for each layer in soil profile with a pooling(averaging) interval of 0.15m. Therefore, data sets for Location A and B(Data Sets A and B) consist of digitized records of vertically pooled data. The resulting data for Location A are shown in Fig. 3a, and also for reference, those for Location B are shown in Fig. 3b.

Many field studies have characterized the population of investigated geotechnical variable in terms of its mean, variance and coefficient of variation. Seldom has the type of frequency distribution of the population been identified. A normal distribution is normally assumed for computational purpose. Lumb(1966), Schultze(1975), and Corotis et al.,(1975) concluded that the physical characteristics of geotechnical properties such as water con-

tent, void ratio, cohesion. and coefficient of consolidation can be approximated by a normal or lognormal distribution.

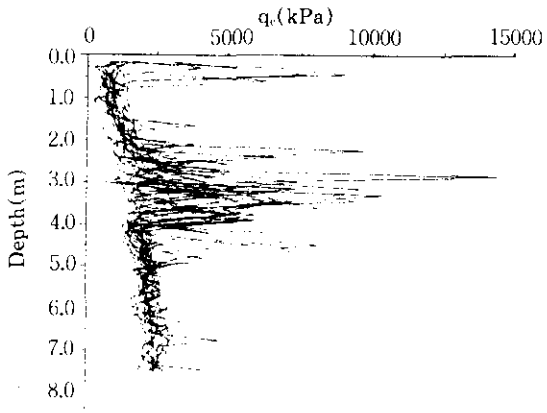

Fig. 3 (a) General variability of 28 CPT q_c profiles for location A

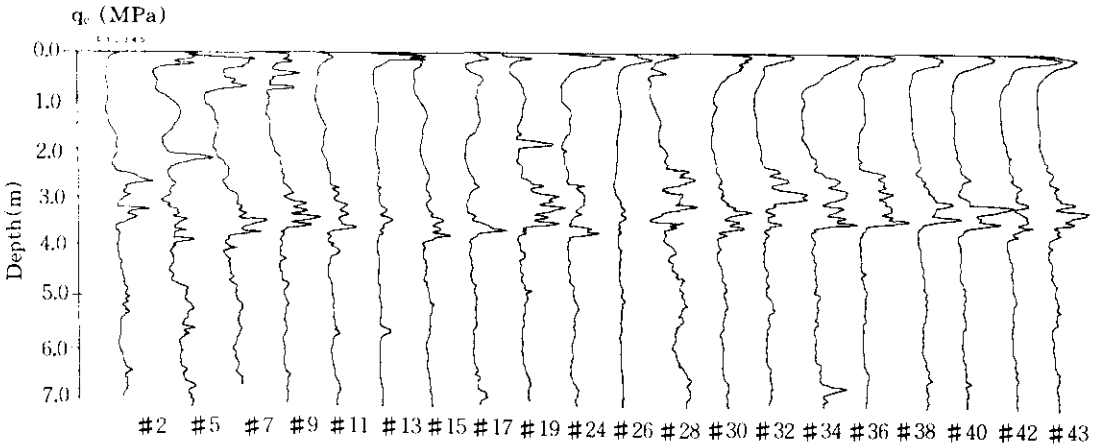

Fig. 3 (b) General variability of 38 CPT q_c profiles for location B

In order to analize q_c data statistically, a histogram of the pooled q_c data from Locations A is plotted in Fig. 4 for Layers 1-3 considered. These data suggest that a log normal distribution of q_c is adequate, although not exact. Also, a typical cumulative frequency plot (probability plots) is shown in Fig. 5. Since this plot approximates straight lines, it can be concluded that q_c data sets in NGES-UH are approximately log normal.

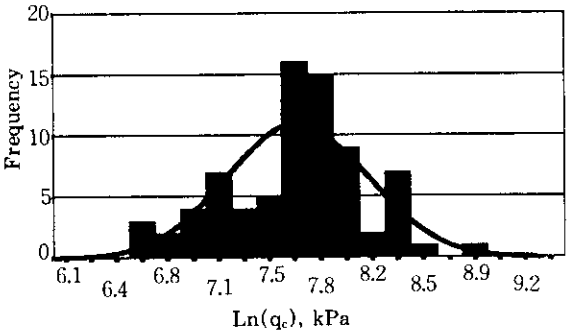

Fig. 4 Histogram of pooled q_c from locations A

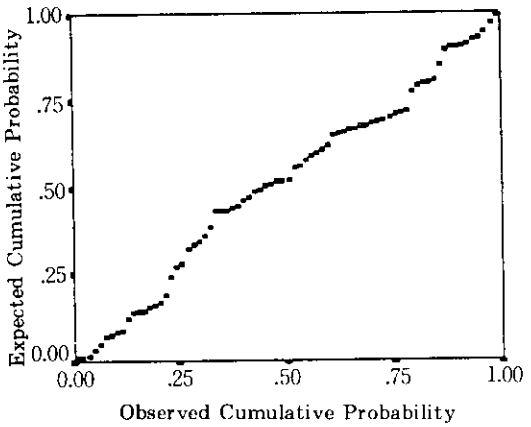

Fig. 5 Cumulative probability for observed data vs. expected cumulative probability for log normality for q_c

According to Ledvina(1991), whether a distribution of interest is normal, log normal, or has some other characteristic in geostatistical analysis, there is no particular geostatistcal significance, except that it is often more difficult to interpret variograms for highly skewed distributions such as the log transformed data. Log normality will therefore be assumed here.

For description purpose, statistical properties of the three layers for normal distribution are given in Tables 1 and 2.

Table 1. Data set A-location A

Layer	Depth(m)	Mean L. L.(%)	Mean P. L.(%)	Mean w(%)	Samples N*	Mean q_c(kPa)	COV
1	0.0 to 2.5	47	14	19	396	1496	0.74
2	2.5 to 3.5	53	16	23	199	3211	0.55
3	3.5 to 7.5	66	21	27	503	2397	0.28

N* Pooled numbers of q_c sample sets
L. L. = Liquid Limit, P. L. = Plastic Limit, w = Water Content

Table 2. Data set B-location B

Layer	Depth(m)	Mean L. L.(%)	Mean P. L.(%)	Mean w(%)	Samples N*	Mean q_c(kPa)	COV
1	0.0 to 2.5	47	14	19	608	1608	0.43
2	2.5 to 3.5	53	16	23	304	2654	0.38
3	3.5 to 7.5	66	21	27	836	2043	0.10

N* Pooled numbers of q_c sample sets
L. L. = Liquid Limit, P. L. = Plastic Limit, w = Water Content
Note : Index properties are for entire site and are not distinguished between Locations A and B

4. Geostatistical Analysis

The geostatisitcal analysis of spatial variability of CPT data performed for NGES-UH consists of four steps: The first step is to investigate if data are additive and normally distributed and to make approximate transformations if they are not. Normal distribution of data is not a requirement for geostatistical analysis. However, normally distributed data will give the best estimates(Christakos, 1992). The second step is to estimate the spatial correlation structure of pairs of measured data. This is accomplished with theoretical variograms. In the third step, a theoretical model is fitted to the experimental variogram, and in the fourth step the fitted model is used in stochastic interpolation, known as kriging.

The first step of the geostatistical study for the q_c data for the NGES-UH was covered in the preceding section. Distribution is assumed to be log normal.

4.1 Constructing a Variogram Models

The most direct way to compare two q_c values, denoted Z(x) and Z(x+h) at two points x and x+h, is to consider the difference in their values. This resulting dissimilarity between values at two points is of little interest, however. A more significant parameter is the average difference between two points, defined as:

$$r(h)=\frac{1}{2}E\{[Z(x+h)-Z(x)]^2\}. \tag{1}$$

Equation 1 is defined as the variogram. E is the expectation of the difference of the variable estimated at x and x plus some distance increment h. However, one needs to consider the value difference, [Z(h)-Z(h+x)], for all possible points x and x+h. At some separation distance h the value Z(x) will be independent of Z(x+h). This point is called the range of influence and is denoted as "a", which represents the distance beyond which the points are no longer correlated.

For mathematical simplicity, one considers the squared difference and selects it as the dissimilarity function. Therefore, the variogram describing the spatial correlation between samples in near proximity is half the average squared difference between pairs of points separated by distance h. r(h) may then be calculated as:

$$r(h)=\frac{1}{2N(h)}\sum_{i}^{N(h)}[Z(x_i+h)-Z(x_i)]^2 \tag{2}$$

where

$Z(x_i)$ represents the value of the data at location x_i,

h is the distance between the data pairs, and
N(h) is the number of couples of observation points in the region.

Equations 1 and 2 assume that the value of r(h) depends only on the separation distance h and not the location x of the sample points. In practice, with limited data, one can compute the variances for groups of pairs of measurements in class intervals of similar distance and direction and then plots a graph of the variance versus distance for a particular direction. A model curve is then fit to the resulting graph: this model is assumed to be an approximation of the true variogram.

There are several possible experimental variogram models, such as the spherical, exponential, and linear models shown in Fig. 6. The nonzero value of r(h) at the origin, h = 0, C(0), in Fig. 6 represents "nugget" effect, which results from a combination of measurement errors, microstructure in the data and small distances between sample pairs. When there is no spatial structure(uncorrelated values) over the range of h, the variogram is modeled as a "pure nugget" effect, as shown in Fig. 6b, which has constant variance. This corresponds to the case of independent(uncorrelated) observations, which is normally attached by a deterministic trend surface approach.

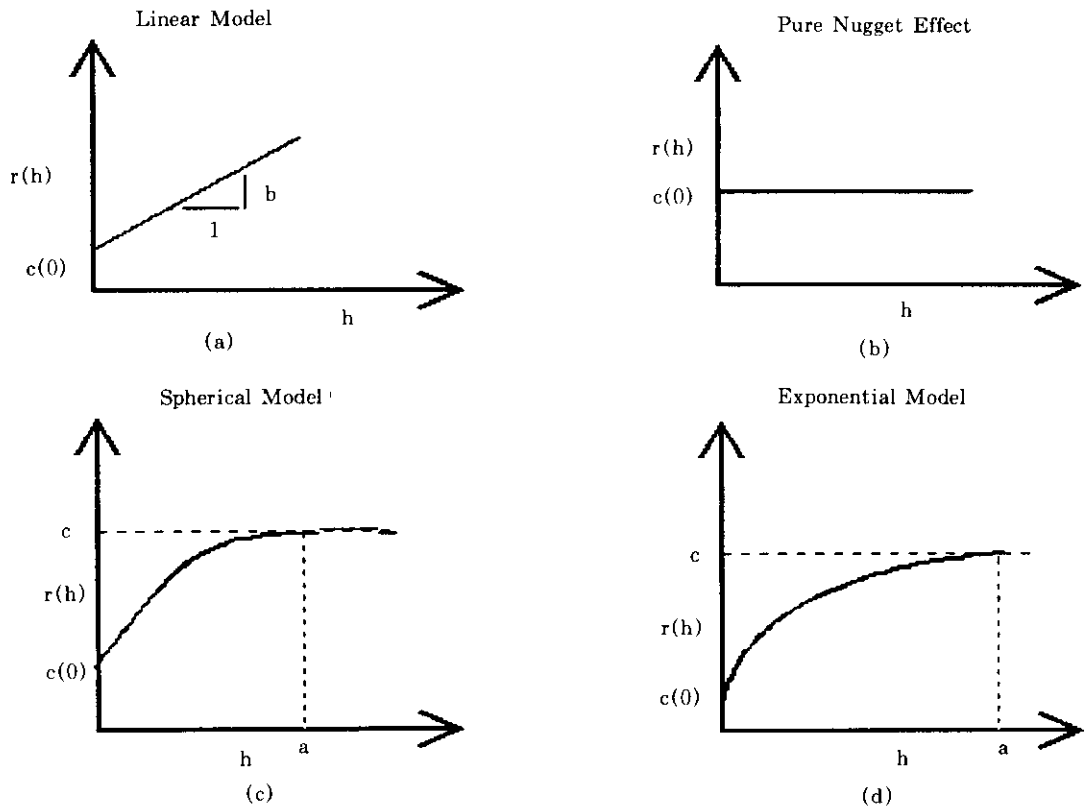

Fig. 6 Theoretical models of variogram.

The spherical model is represented mathematically by:

$$r(h) = C(0) + C[\,1.5h/a - 0.5(h/a)^3\,] \quad \text{when } h \le a, \tag{3}$$
$$= C(0) + C, \quad \text{when } h \ge a,$$

and where

C(o) is the nugget effect,
C is the "sill" of the variogram,
a is the range of the influence of a sample, and
h is the "lag" or distance between sample pairs.

This model was originally derived on theoretical grounds but has been found to be widely applicable in practice.

Another model is the exponential model. This model is described by:

$$r(h) = C(0) + C[\,1 - \exp(h/a)\,]. \tag{4}$$

In this model r(h) rises more slowly from the origin than in the spherical model and never quite reaches its sill.

The simplest of variogram model is the linear model:

$$r(h) = bh, \tag{5}$$

where

b is the slope of the variogram line.

The interpretation of the linear variogram is that the variability between two observations increases linearly as the distance between them increases. This shape represents a continuous but not a differentiable random field and a parameter (q,c) with an irregular structure or non-homogeneous spatial structure(Isaaks and Srivastava, 1989). More theoretical discussion of variogram models is beyond the scope of this paper. The reader may refer to Journel and Huijbregts(1963).

Using the 28-CPT data set at Location A and the 38-CPT data set at Location B, experimental variograms have been developed and fitted by theoretical variogram in Figs. 7-8. The variograms for Location A are omni-directional, which allows all pairs to be included regardless of direction, because of the randomly-sampled data. For Location B unidirectional variograms have been developed. Generally omni-directional variograms maximize the number of pairs in each distance class, which gives the best or smoothest variogram.

4.2 Results of Variogram Analysis

Vertical variogram models of Locations A and B are shown in Fig. 7. They possess good continuity with a periodic cyclicity, hole effect, caused by geological formation and were fitted with a spherical model. Vertical correlation distance determined from experimental variograms for Locations A and B are 2.5m and 1.5m, respectively. These values are reasonable because the first is from omni-directional data, and the second is from unidirectional data. From these variograms, it seems reasonable to mention that Locations A and B have quite similar data structure(same trend), which means that two locations are not very different in vertical formation structure.

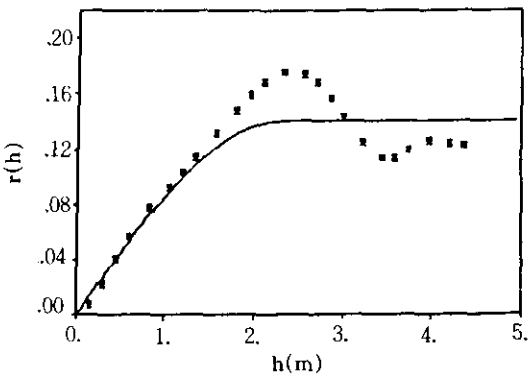

Fig.7 (a) Vertical variogram for location A

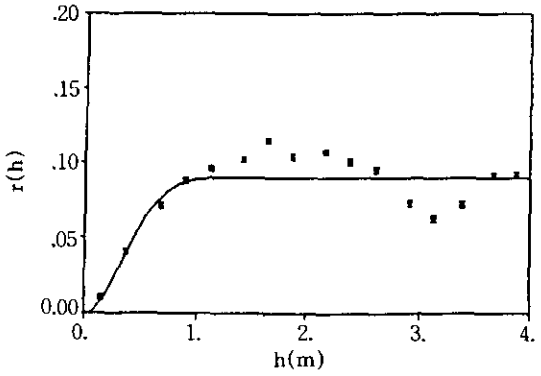

Fig.7 (b) Vertical variogram for location B

The horizontal variograms of Layers 1, 2, and 3 for Location A are shown in Fig. 8. The variogram for Layer 1, from the ground surface to a depth of 2.5m, is quite erratic, but fitted exponentially, with a correlation distance of 3 m. In Layer 2 the variogram exhibits almost a pure nugget effect describing no correlation between data. For Layer 3, a spherical variogram is fitted, with a 10 m horizontal correlation distance.

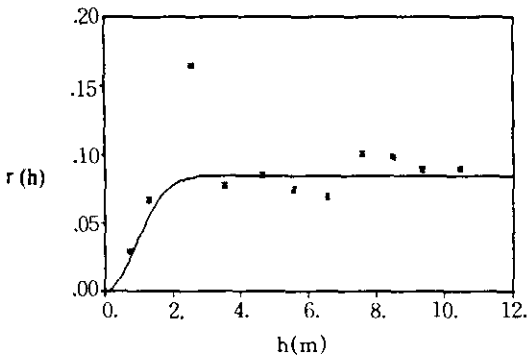

(a) Layer 1

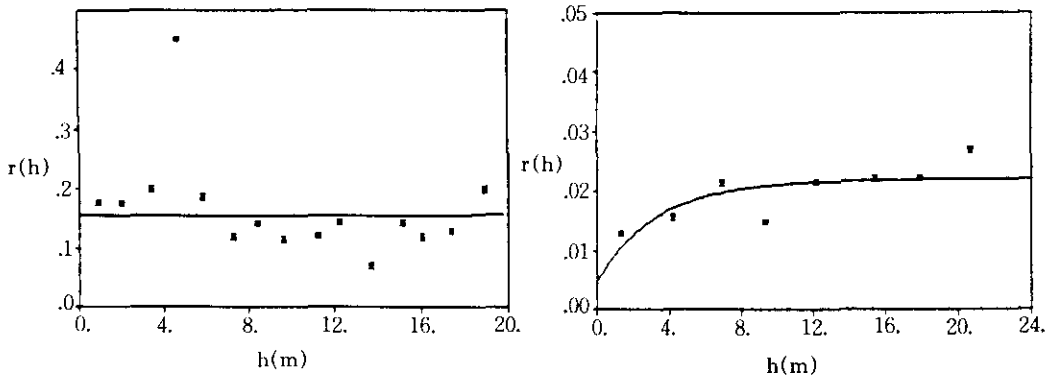

(b) Layer 2 (c) Layer 3

Fig. 8 Horizontal variograms for layers 1, 2 and 3(Location A)

Horizontal variograms for Location B are also shown in Fig. 9. Layer 1 exhibits a spherical variogram with a 4 m correlation distance, but there exists an erratic and periodic trend. In Layer 2, the linear variogram models the data reasonably, with a 20 m correlation distance. In Layer 3, a spherical variogram is fitted, with a 9 m correlation distance.

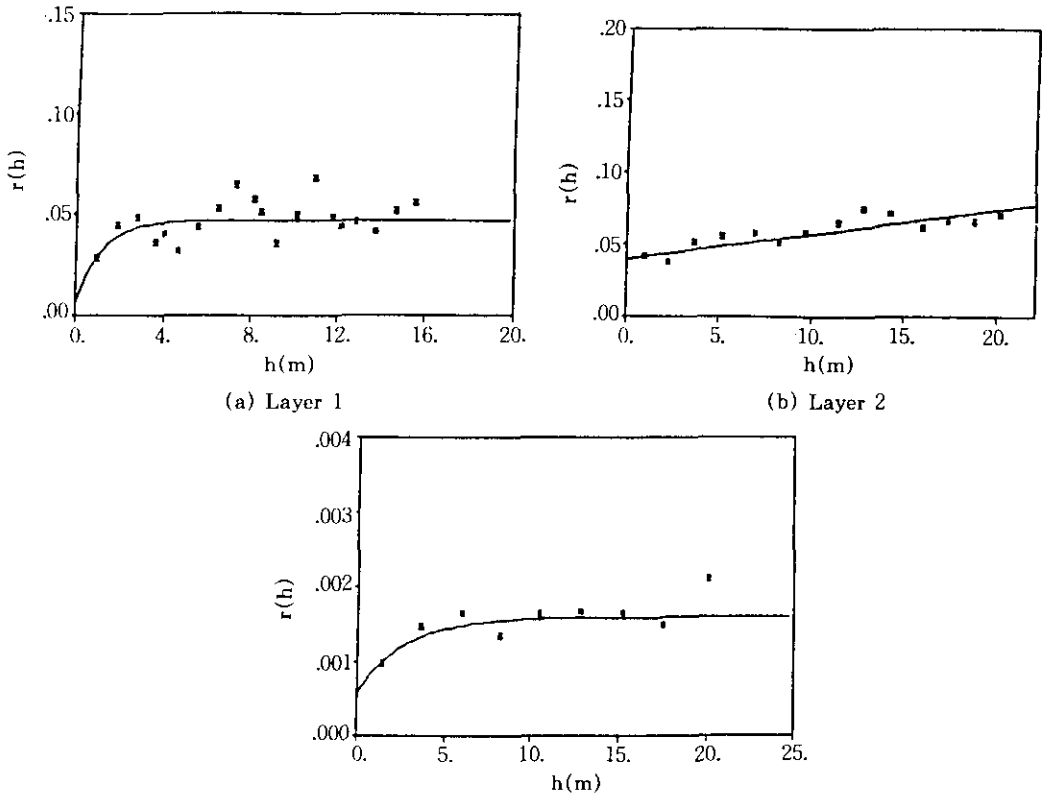

(a) Layer 1 (b) Layer 2

(c) Layer 3

Fig. 9 Horizontal variograms for layers 1, 2 and 3 for location B.

Horizontal variogram models for the Locations A and B shown in Figs. 8-9 are relatively in a good agreement in layers 1 and 3 but somewhat different in layer 2 even though omni-directional variogram in Location A and unidirectional variogram in Location B have been applied to fit true models. However, there is some difference in variance in corresponding layers between Locations A and B. The variances for layers 1-3 in Location A are larger than those of Location B. These differences are due to different sampling methods(Random sampling in Location A and consistent sampling in Location B). From the comparison of these variograms, it seems also reasonable to mention that Locations A and B have similar data structure, which means that two locations are not very different in the geological formation of horizontal structure.

4.3 Kriging

A primary objective of a site investigation is to increase the reliability of the estimation of spatial variability of the soil property or properties of interest. If zones in three-dimensional space in which high uncertainty in the property of interest can be identified, additional testing can be directed to those zones to reduce the uncertainty. If a designer follows effective programs to reduce uncertainty in the soil evaluation in a systematic manner, resistance factors in foundation design can be increased, or factors of safety can be reduced. One technique that can be used for this purpose is "kriging", so called [Isaaks and Srivastava, 1989) because it was first applied by a South African mining engineer by the name of D. G. Krige. To demonstrate its applicability to design, the kriging method was applied to the q_c data from the NGES-UH as follows. Layers 1-3 were identified, and at each location at which a cone sounding was made a depth-averaged or "pooled" value of q_c ("observation") was computed for each layer. Estimated values for pooled q_c, termed $Z^*(x_o)$, were then computed at any particular point xo on an x-y grid for each of the three layers at Location A, using Eq. 6.

$$Z^*(x_o) = \sum W_i Z(x_i) \tag{6}$$

W_i is a weighting factor for every i-th observed value in the layer, $Z(x_i)$. For every position x_o at which an estimated value(Z^*) is calculated, the weighting functions for the values at the observation points are computed by using the ordinary kriging principles that (a) the mean value of $[Z^*(x_o)-Z(x_o)]$ at all points in the domain must be zero, where $Z(x_o)$ is the unknown real value, and (b) the estimation variance, $[Z^*(x_o)-Z(x_o)]^2$, must be minimized. Consideration of these principles leads to the kriging equations:

$$\sum_{j=1}^{N} W_j r(x_i, x_j) + \mu = r(x_i, x_j), \tag{7}$$

$$\sum_{j=1}^{N} W_j = 1 \tag{8}$$

In the kriging equations the functions r are the variogram functions that have been developed previously for the layer being evaluated between any two observation points x_i and x_j which are assumed to apply between each observation point x_i and the estimation points x_0. The factor μ is a Lagrangian multiplier. Equations 7 and 8 are solved simultaneously to obtain the values of W_i and μ corresponding to any estimation point x_0(Eq. 6), and $Z^*(x_0)$ is evaluated. The process is repeated for every grid point in the layer and for each of the layers.

The procedure for finding set of weights is complex enough that one needs a computer. For this study, the geostatistical software GEO-EAS, developed by the U.S. Environmental Protection Agency (Englund and Spark, 1991), was used to create and model the variograms for Locations A and B.

Figure 10 shows the surfaces of q_c for Layers 1-3 in Location A. These kriged surfaces have been developed by using 24 pooled data points for Layer 1, and 26 for Layers 2 and 3.

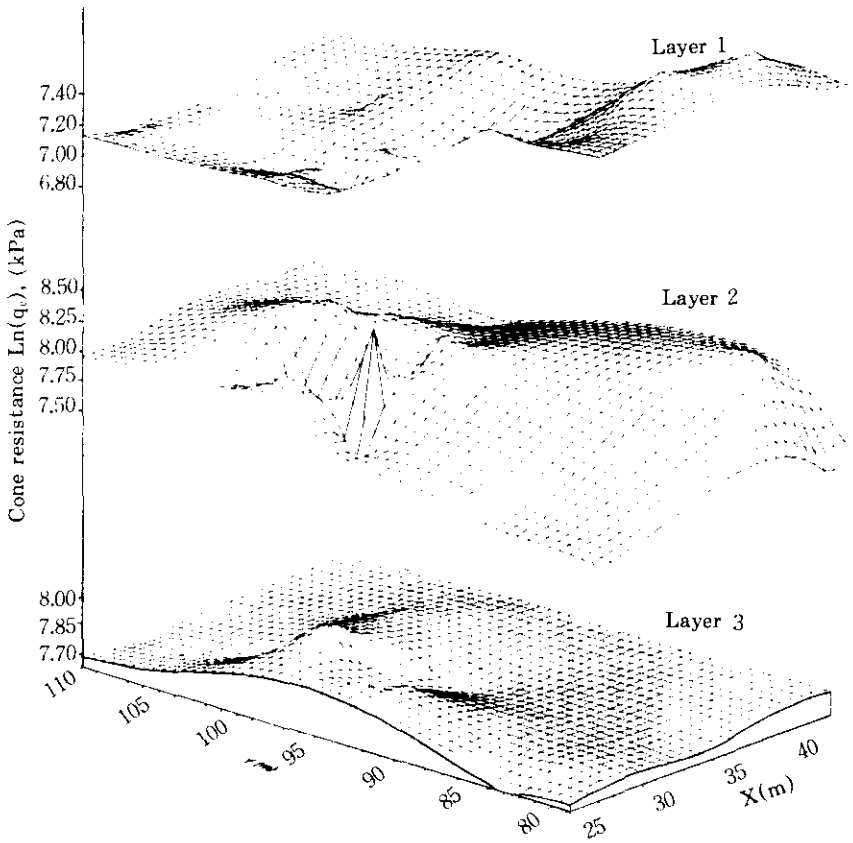

Fig. 10 Surface plots describing spatial variability of q_c (Location A)

Only the variograms for Location A(Fig. 8) were used for these constructions. The surface plots for Layers 1 and 2 indicate that unmeasured points are estimated with minimum error and unbiased condition, which means that the kriging surfaces best estimate the variation of q_c in each layer. Fig. 10 shows high spatial variability of q_c in Layers 1 and 2, while Layer 3 exhibits a small variation of q_c within the blocked area. These facts reflect high variability in the surface layers, which have been highly weathered. Relatively higher variation appears in Layer 2, due mainly to a thin seam of mixed material(fine sand and clay) that is unweathered, and a low variability appears at Layer 3, which is an unweathered and visually a relatively homogeneous clay formation.

Kriging surfaces showing Z^* the best estimate,(in this case the natural logarithmic of q_c) vs. horizontal (x, y) position on the site are shown for Layers 1-3 in Fig. 10. The value of q_c is expressed in logarithmic form because the probability distribution of the data for constructing the variograms has been assumed to be log normal. Observation of this specific figure for the NGES-UH reveals that the most consistent data are in Layer 3, but that an anomaly exists in that layer near $x = 30$ m, $y = 100$ m. This information suggests, for example, that drilled footing foundations formed in this layer can be designed with higher resistance factors than shallow footings in the upper two layers but that additional soundings in the vicinity of 30, 100 are desirable.

Three-dimensional, topographic representations such as those shown for the NGES-UH give the designer a clear picture of the variation of the design parameter, in this case q_c, throughout the site, and enable him to easily select the most appropriate value of the design parameter for locations at which samplings have not been made. With this information the designer is also in an improved position to recommend locations for additional subsurface investigations and to assess foundation safety.

5. Discussion and Conclusions

The geostatistical method described in this paper was found to be very useful to estimate the spatial variation of cone resistance (q_c) and to determine vertical and horizontal correlations systematically. The range of correlation distance derived from variograms is reasonable for Locations A and B. These results have important implications in sampling programs because if one needs to compare two test results, sampling must be made within these vertical or horizontal correlation distances. The NGES-UH, like other NGES's in the U. S., may be used to compare the performance of *in situ* testing instruments. In order to make meaningful comparisons at this site in Layers 1-3, side-by-side comparisons must be made within the horizontal and vertical correlation distances that have been determined, for example, 9 m horizontally and 1.5 m vertically in Layer 3 at Location B, which is a Location set aside for *in situ* test research.

The nugget effect exists in the horizontal direction for both Locations A and B, while no

nugget effect exists in the vertical variograms for either location. The nugget effect is produced by one of the following factors: inherent soil variability at a small scale and measurement errors. It seems reasonable to decide that the main factor producing the nugget effect in the horizontal variograms is small-scale variability, which is consistent with the geological history of the site.

Three-dimensional kriging plots, which indicate the best estimates of unsampled points for randomly sampled Location A, provide a clear understanding of spatial variability of q_c. This information can be used for optimal sampling design, with an indication of further site investigation, establishing for safe design loads, and for determining maximum separation distances for comparing *in situ* test results.

Acknowledgments

The study reported here was funded in part by an umbrella grant for the United States NGES system, administrated by the University of New Hampshire, and ultimately supported by the National Science Foundation and the Department of Transportation. Most of soundings were performed with the help of Fugro Geosciences, Inc., and its predecessor companies, from 1979 to 1994. The authors gratefully acknowledge their significant contribution to the acquisition of high-quality data.

Finally, the first author would like to thank for very helpful review and suggestions to reviewer.

References

1. Anderson, L. R., Sharp, K. D., Bowles, D. S., and Canfield, R. V, (1984), "Application of Methods of Probabilistic Characterization of Soil Profiles," Probabilistic Characterization of Soil Properties, Bridge Between Theory and Practice, Proceedings of the ASCE Convention, Atlanta, Georgia, USA. eds. D. S. Bowles and H. Y. Ko., pp. 90-105.
2. Baecher, G. B., (1983), "Geostatistics, Reliability and Risk Assessment in Geotechnical Engineering," Geostatistics for Natural Resources Characterization, Part 2, NATO Series C, PP. 731-744.
3. Campanella, R. G., Wickremesinghe, D. S., and Echezuria, H. J., (1989), "Cone Penetration Test for Site Characterization," Twelfth International Conference on Soil Mechanics and Foundation Engineering(ICSMFE), Rio De Janeiro, Brazil, pp. 205-210.
4. Christakos, G., (1985), "Modern Statistical Analysis and Optimal Estimation of Geotechnical Data," Journal of Engineering Geology, Vol. 22, pp. 175-200.
5. Christakos, G., (1992), Random Field Models in Earth Sciences, Academic Press, Inc.
6. Corotis, R. B., Azzouz, A. S., and Krizek, R. J., (1975), "Statistical Evaluation of Soil Index Properties and Constrained Modulus," Proc. of the 2nd Int. Conf. on Application of Statistics and Probability in Soil and Structural Engineering, Vol. 2, Aachen.
7. Englund, E., and Spark, A., (1991), Geostatistical Environmental Assessment Software, User's Guide, U. S. EPA, Environmental Monitoring Systems Laboratory, Las Vegas.
8. Isaaks and Srivastava, (1989), An Introduction to Applied Geostatistics, Oxford University Press,

New York.

9. Jaksa, M. B. Kaggwa, W. S., and Brooker, P. I., (1993), "Geostatistical Modeling of the Spatial Variation of the Shear Strength of a Stiff, Overconsolidated Clay," Probabilistic Methods in Geotechnical Engineering, pp. 186-193.
10. Journel, A, G. and Huijbregts, C. J., (1978), Mining Geostatistics, Academic Press, NY, USA.
11. Ledvina, C. T., (1991), "Geostatistical Inference and Exploration of Coal Mine Roof Strata," Ph. D. Dissertation, Department of Civil Engineering, Northwestern University, December.
12. Lumb, P., (1966), "The Variability of Natural Soils," Canadian Geotechnical Journal, Vol. 3, No. 2, pp. 74-97.
13. Mahar, L. J., and O'Neill, M. W., (1983), "Geotechnical Characterization of Desiccated Clay," Journal of the Geotechnical Engineering, ASCE, Vol. 109, No. 1, Jan., pp. 56-71.
14. O'Neill, M. W., and Yoon., Gil, (1996), "Some Engineering Properties of Overconsolidated Pleistocene Soils of the Texas Gulf Coast," Transportation Research Record, 1996, January.
15. Schultze, E., (1975), "Some Aspects Concerning the Application of Statistics and Probability of Foundation Structures," Proc. of the 2nd Int. Conf. on Application of Statistics and Probability in Soil-and Structural Engineering, Vol. 2, Aachen.
16. Soulie, M., (1983), "Geostatistical Application in Geotechnics", Geostatistics for Natural Resources Characterization, NATO Series C, Part 2, pp. 703-729.
17. Tang, W. H., (1979), "Probabilistic Evaluation of Penetration Resistance," Journal of the Geotechnical Engineering Division, ASCE, Vol. 105, pp. 1173-1191.
18. Vanmarke, E. H., (1977), "Probabilistic Modeling of Soil Profiles," Journal of the Geotechnical Engineering Division., ASCE, Vol. 103, No. GT 11, pp. 1227-1246.

(접수일자 1996. 2. 12)